Crystal Nucleation without Supersaturation

T. Kovács,[1] F. C. Meldrum[2] and H. K. Christenson[1,*]

[1]School of Physics and Astronomy and [2]School of Chemistry
University of Leeds, Leeds LS2 9JT, United Kingdom

* corresponding author
h.k.christenson@leeds.ac.uk

PHYSICAL SCIENCES
Chemistry

Manuscript under review by

Proceedings of the National Academy of Sciences of the U.S.A.

Ref 21 of the FD159 submission

Abstract

Classical nucleation theory has been employed to interpret nucleation phenomena for some eighty years and postulates the formation of an ordered crystalline nucleus directly from vapour or solution. Recently, however, a new "two-step" mechanism of crystal nucleation has been identified which explains how crystallization via a more concentrated, fluid-like phase can lead to significant enhancement of nucleation rates. Here, we provide the first experimental demonstration that a two-step mechanism can accelerate deposition of crystals from vapour. Crucially, this occurs without supersaturation of the vapour phase, which according to CNT should be impossible. The process relies on condensation of supercooled liquid in surface cavities below the melting point. Crystals then nucleate in this liquid, leading to rapid deposition of more solid. Such a mechanism has been postulated for atmospheric nucleation of ice on aerosol particles and shows analogies with processes such as the crystallization of biominerals via amorphous precursor phases.

Introduction

Classical nucleation theory (CNT) describes nucleation processes and how they depend on factors like supersaturation, absolute concentrations and for heterogeneous nucleation, on interactions with the surface. It predicts a free energy barrier to nucleation due to the cost of creating an interface between the old and the incipient phase. Although there are often large quantitative discrepancies between the theoretical predictions and experimental measurements, CNT is still useful as a starting point for the consideration of nucleation problems. However, it is becoming increasingly clear that many nucleation processes do not conform to the classical model, which relies on a sufficient number of molecules coming together to form a nucleus that immediately adopts the structure of the new phase. In its place, experiments and computer simulations have shown that crystal nucleation is mediated by denser fluid precursor phases(1-7) or clusters of molecules(8, 9) from which the final crystal forms. It has been shown both experimentally and theoretically that such two-step mechanisms may lead to a significant enhancement of nucleation rates of proteins and colloids as well as smaller molecules.(5, 7, 8)

Crystallisation of solid from vapour is typically associated with a much larger free energy barrier than crystallisation from solution or from the melt as the free energy of a solid surface in vapour is unusually high. The nucleation of crystals from vapour is therefore particularly unfavourable even when occurring on surfaces, and ice nucleation on solid aerosols in cirrus clouds,(10) for example, requires supersaturation of the vapour phase by 20-50 %. However, according to CNT substrate geometries such as surface cavities, which increase the substrate-nucleus area at the expense of the vapour-substrate area, are expected to facilitate nucleation.(11, 12)

As liquids usually have lower surface energies than solids, it is often observed that solid deposits on a substrate from vapour via an undercooled liquid. Considering again the effect of surface geometry, surface cavities can also facilitate liquid condensation as there is rarely an energy barrier towards condensation in an acute wedge, and it occurs even from undersaturated vapour. This process is termed capillary condensation and also take place below the bulk melting temperature T_m as the smaller interfacial free energy between the substrate and liquid than between the substrate and a crystal favours the liquid over the solid state.(13, 14) These liquid condensates cannot then grow indefinitely, even at saturation, as there cannot be equilibrium between saturated vapour and bulk liquid below T_m. Indeed, the radius of curvature r of the liquid-vapour interface in *saturated* vapour is inversely proportional to the temperature depression ΔT below T_m ($\Delta T = T_m - T$, the actual temperature) and for small ΔT is given by(14)

$$\frac{1}{r} = \frac{\Delta H_{fus} \Delta T}{V_{ML} \gamma_{LV} T_m} \qquad (1)$$

where γ_{LV} is the surface energy of the liquid, V_{ML} its molar volume and ΔH_{fus} its enthalpy of fusion (inclusion of the temperature dependence of the surface tension and the enthalpy of melting leads to a more complicated relationship).(14)

Consequently, in a conical or wedge-shaped pore a liquid condensate can only grow until its liquid-vapour interface satisfies the condition of eq. 1. A simple analysis also shows that a region of the condensates next to the liquid-vapour interface is metastable towards freezing as long as the surface tension γ_{LV} is more than twice as large as γ_{SL}, the interfacial tension between the liquid and its solid, a condition which is easily satisfied for most common substances.(14) If this region were to crystallise or freeze, this could provide an alternative

route to the deposition of solid from vapour, since once crystals have formed these can grow indefinitely in saturated vapour below T_m. Clearly, this would lead to greatly enhanced rates of crystal nucleation from vapour *as no supersaturation is required*.

In this article we investigate the viability of this mechanism as a means of achieving greatly enhanced deposition of solid from vapour by removing the requirement for supersaturation. 3 contrasting model substances having T_m above room temperature, and reasonably high saturation vapour pressures p_{sat} at room T were selected for study: hexamethylcyclotrisiloxane (HMCTS); p_{sat} (25 °C) = 5 mm Hg,(15) T_m = 64.5 °C,(16) *neo*-pentanol; p_{sat} (25 °C) = 16 mm Hg,(17) T_m = 52.5 °C,(16) and norbornane; p_{sat} (25 °C) = 28 mm Hg,(18) T_m = 87.5 °C(16)).

Results

The investigation was carried out using a simplified(19, 20) surface force apparatus that has previously been used in a range of capillary-condensation experiments. In the experiments two curved (radius of curvature R = 2 cm) mica surfaces in a crossed-cylinder configuration, are brought into contact in saturated vapour in a sealed, temperature-controlled chamber. The surfaces are pulled into contact (separated by a few molecular layers) from separations of 10-20 nm by the negative Laplace pressure in a liquid capillary condensate,(20) which forms by a film-thickening mechanism.(21) These jump distances are typical of substances below T_m where only about two molecular layers are adsorbed on isolated surfaces.(14, 22) Thicker films above T_m may give rise to much larger jumps.(21) As they come into contact the mica surfaces flatten (Figure 1) due to their large R and the relatively soft glue used to mount them.(23) The flattened mica surfaces in contact form an annular wedge in which liquid will condense from the saturated vapour until the separation h between the mica surfaces at the

liquid-vapour interface is approximately twice the interfacial radius of curvature given by eq. 1 (see Methods section).

Capillary condensation of all three substances from saturated vapour was studied as a function of ΔT and there are three regimes of behaviour. For undercoolings of $\Delta T \leq 18$ K (*neo*-pentanol) or $\Delta T \leq 33$ K (HMCTS) a liquid condensate of limited size initially forms around the contact zone (Figure 2 a-c). That the condensate is liquid is demonstrated by separating the surfaces, in which case the diameters of both the flattened contact area and the liquid condensate decrease smoothly until the surfaces come apart and the annulus turns into a bridging neck, which quickly evaporates (Figure 2c). No liquid condensates can be observed with norbornane as the minimum undercooling achievable with our system is 37 K.

At the largest undercoolings ($\Delta T > 34$ K) the behaviour is very different, and with all three substances a condensate grows rapidly immediately after the surfaces come into contact (Figure 3d). Condensate sizes, *h* (as defined in Figure 1) of between 200 nm (HMCTS) and 2 μm (norbornane) were observed within 30 min. The contact diameter of the surfaces cannot be changed by loading or unloading, but instead, the surfaces deform beyond the condensate (Figure 2e). The force required to separate the surfaces is about an order of magnitude larger than with the liquid condensate. This shows that the condensate is solid, and "glues" the surfaces together. On separation, an annular deposit of material is left on both surfaces (Figure 2f), and this evaporates over seconds to minutes, since the vapour is not supersaturated.

At intermediate temperatures ($18 < \Delta T < 30$ for *neo*-pentanol, and at $\Delta T \approx 34$ K for HMCTS) the initial condensate is liquid, but rapid deposition of material is frequently observed, likely

in response to an external stimulus (e.g. vibration). Alternatively, rapid deposition can be induced by increasing the load slightly – which perturbs the surfaces – and then unloading the surfaces. This rapidly depositing material is clearly solid, as explained above, although the innermost region of the condensate almost certainly remains liquid, as expected on theoretical grounds.(14, 24)

The substantial difference in size between the solid deposits (filled symbols) and liquid condensates (open symbols) is shown in Figure 3 (plotted as 1/r vs ΔT, although the solid-vapour interface is not necessarily curved like a liquid-vapour interface). The agreement with theory for the interfacial radius of curvature r ($\approx h/2$) of the liquid condensates is very good (solid lines). The error bars for HMCTS are large as the condensate is too small for its size to be directly measured with the surfaces in contact and it can only be estimated from the size of the liquid neck immediately after separation of the surfaces. With norbornane only very large solid condensates are observed at $\Delta T > 37$ K. The solid condensate is also visible in a microscope by observing the mica surfaces from above (Figure 4) which enables the process of separation to be followed. As the surfaces come apart the solid norbornane condensate shatters into fragments which then evaporate, confirming that the vapour phase is not supersaturated. Finally, that this route to nucleation is not surface-specific is shown by the formation of analogous solid deposits around the contact point of crossed cylinders of amorphous silica – the material of the cylindrical discs that normally support the mica sheets.

Discussion

Our results demonstrate convincingly and conclusively that deposition of crystals may occur from vapour without supersaturation. The requirement is a wedge-shaped cavity which allows the capillary condensation of liquid below T_m. The observed undercoolings of the studied substances are similar to those reported for homogeneous nucleation from the melt in water, where experimental values of the nucleation rate at ΔT = 35 K vary from 10^{11} to 10^{13} $m^{-3}s^{-1}$ and from 10^{13} to 10^{15} $m^{-3}s^{-1}$ ΔT = 38 K.(25) The volume V of the annular capillary condensates is approximately πRh^2,(26) so V ~ 10^{-17} m^3 for ΔT = 35-38 K, which would give nucleation times of the order of μs – ms. Our results could hence be explained purely in terms of classical homogeneous nucleation of solid in the liquid capillary condensates. However, in view of the large uncertainties involved we cannot rule out heterogeneous nucleation of crystals on the mica surface, or some enhancement of nucleation rates due to the presence of a three-phase line, as has been shown experimentally(27) and in computer simulations(28)

Although performed with model compounds, these results are highly relevant to many crystallisation phenomena. The atmospheric nucleation of ice on solid aerosol particles has been proposed to occur via capillary condensation of supercooled liquid water in surface cavities,(29, 30) and our results now show that this may indeed be a viable mechanism. Given that atmospheric nucleation of ice on aerosol particles is a major determinant of the earth's climate the importance of such a route to nucleation cannot be understated. It has also been shown that nanoscale pits or pores can enhance nucleation rates of proteins(4, 31, 32) and small molecules,(33) particularly when the interactions between the nucleating substance and the surface are favourable. A simulation study has discussed this enhancement in terms of capillary condensation of fluid in surface pits,(34) in direct analogy with what we have

now demonstrated. Since crystallisation of proteins is a prerequisite for structure determination with diffraction techniques pathways which enhance nucleation rates are of great importance to medicine and biology.

Simulations of colloidal particles have shown that nucleation rates in systems with short-range attractive interactions are greatly enhanced by the presence of a metastable fluid-fluid separation.(1) This fluid-fluid phase separation is a remnant of the phase separation into a dilute vapour-like phase and a more concentrated liquid-like phase that is found in colloidal systems with longer-range attractions. This has been experimentally demonstrated for globular proteins(2, 3) and small organic molecules.(8, 9) In our experiments metastable capillary condensates are stabilised by confinement in a surface cavity at temperatures where the bulk vapour-to-liquid transition does not occur. There is an obvious analogy with the metastable fluid phase in the colloidal systems. A similar phenomenon in homogeneous nucleation has been suggested by recent computer simulations showing that crystal nucleation from vapour may proceed *via* liquid precursor droplets.(35, 36)

In summary, nucleation and subsequent rapid growth of crystals will occur in liquid capillary condensates formed from saturated vapour at undercoolings equivalent to those required for bulk liquids to freeze by homogeneous nucleation. Deposition of crystals from vapour is hence possible without any supersaturation of the vapour phase given the appropriate surface topography. Although this has been the subject of theoretical discussions, we believe that our work for the first time confirms this experimentally. Similar models have been successfully used to explain important phenomena such as protein crystallisation, and it is intriguing whether nucleation rates in many other processes, such as the formation of crystalline biominerals like calcite and hydroxyapatite via an amorphous phase(37), may also be enhanced by a two-step process. Recent discoveries of amorphous precursor phases in several

other systems(38, 39) can only serve to increase the possible importance of this type of two-step process.

Methods

Muscovite mica (Paramount Corp., N.Y.) was cleaved to 2-5 μm thickness, cut into ~1 cm^2 sheets with a white-hot Pt wire, and coated with 50 nm of Ag by thermal evaporation at p = 10^{-6} mm Hg. Two such mica sheets were glued with the silvered side down on silica discs (radius of curvature R = 2 cm) with an epoxy resin (Epikote 1004). The discs were mounted in a crossed-cylinder configuration with the lower disc attached to a rigid support (spring constant > 10^5 Nm^{-1}) to minimise spring deflection inside the stainless steel chamber of a simplified(19, 20, 40) Mark IV SFA. When white light is passed through the opposing, back-silvered mica surfaces only discrete wavelengths are passed by this multiple-beam interferometer.(41) These fringes of equal chromatic order (FECO) were recorded with a CCD camera at the exit slit of a monochromator and the standard three-layer interferometry equations employed to give the surface separation with an accuracy of ca. ± 0.2 nm.

The SFA was housed in a wooden enclosure whose temperature may be controlled with Peltier elements. Measurements in N_2 gas at T = 22 °C were carried out to determine the zero of surface separation (mica-mica contact). A few g of the substance (hexamethylcyclotrisiloxane, *neo*-pentanol or norbornane) to be studied was then introduced into the chamber to saturate the atmosphere. Establishment of equilibrium was assumed when experimental observations on subsequent days were identical (this usually took 3-4 days). During a typical experimental run the surfaces were brought together slowly (a few nm s^{-1}) with a piezoelectric positioner until they jumped together due to capillary condensation, the growth of the capillary condensate with time was monitored and the behaviour on increasing

and decreasing the load as well as on separation of the surfaces determined. After a suitable number of repeat cycles the surfaces were separated and the temperature changed. Equilibration at each new temperature was typically done overnight. The temperature was measured with an accuracy of ± 0.1 ^{o}C with a Pt-resistance thermometer (checked against a water-ice mixture) positioned inside the chamber, about 2 cm from the surfaces,

Refractive index discontinuities in the FECO allowed determination of the condensate size *h* (Figure 1). *h* is related to the radius of curvature of the condensate (*r*) and thickness (*t*) of the adsorbed water film on the surfaces by $h = 2r + 3t$.(42) Based on previous experiments with t-butanol(22) and cyclohexane(14) we used $3t$ = 2 nm as a reasonable correction, although the exact value of this correction is numerically unimportant in the experiments presented here. The magnitude of total radius of curvature *r* of the interface of the condensate is given by (Figure 1).

$$\frac{1}{|r|} = \left|\frac{1}{r_1} + \frac{1}{r_2}\right| \approx \frac{1}{|r_1|} \qquad (2)$$

where r_1 and r_2 are the principal radii of curvature of the condensate. Since $|r_2|$ is of the order of tens of microns and $|r_1|$ is 10 - 1000 nm the approximation in eq. 2 introduces negligible error. We have plotted condensate radii rather than the size as it is the radius which can be directly related to ΔT, even if the significance of interfacial radius is not clear if the condensate is solid.

Acknowledgments

HKC and TK thank the Leverhulme Trust (grant F/10 101/B) and FCM thanks the EPSRC for financial support.

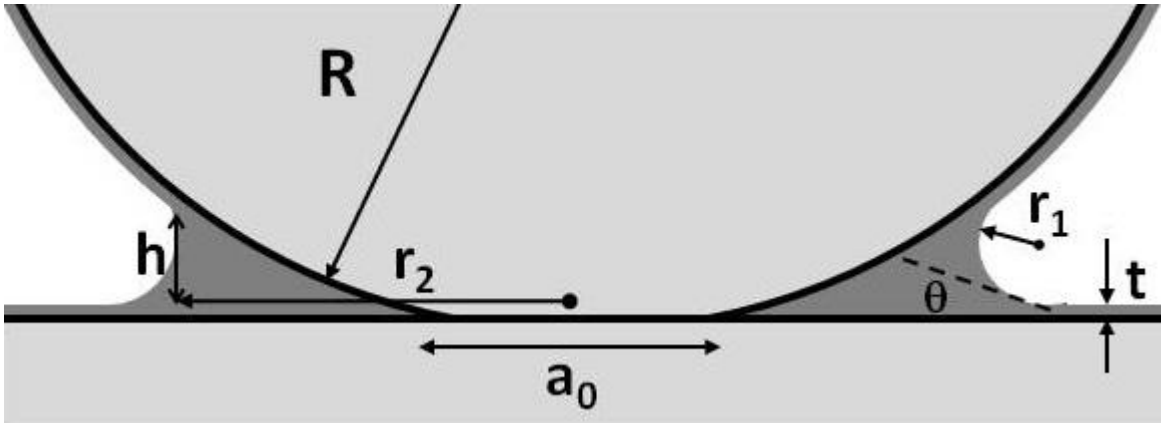

Figure 1 Schematic cross-section of crossed-mica cylinders shown in the equivalent sphere-on-a-flat configuration, with a liquid capillary condensate around the flattened contact region. Typically, R = 2 cm, a_0 ~ 25 μm, r_2 ~ +13-50 μm, $h/2 = r_1$ ~ -(5 nm- 1 μm). h is related to the radius of curvature of the vapour-condensate interface (r) (for liquids) and thickness (t) of the adsorbed film on the surfaces by $h = 2r + 3t$.

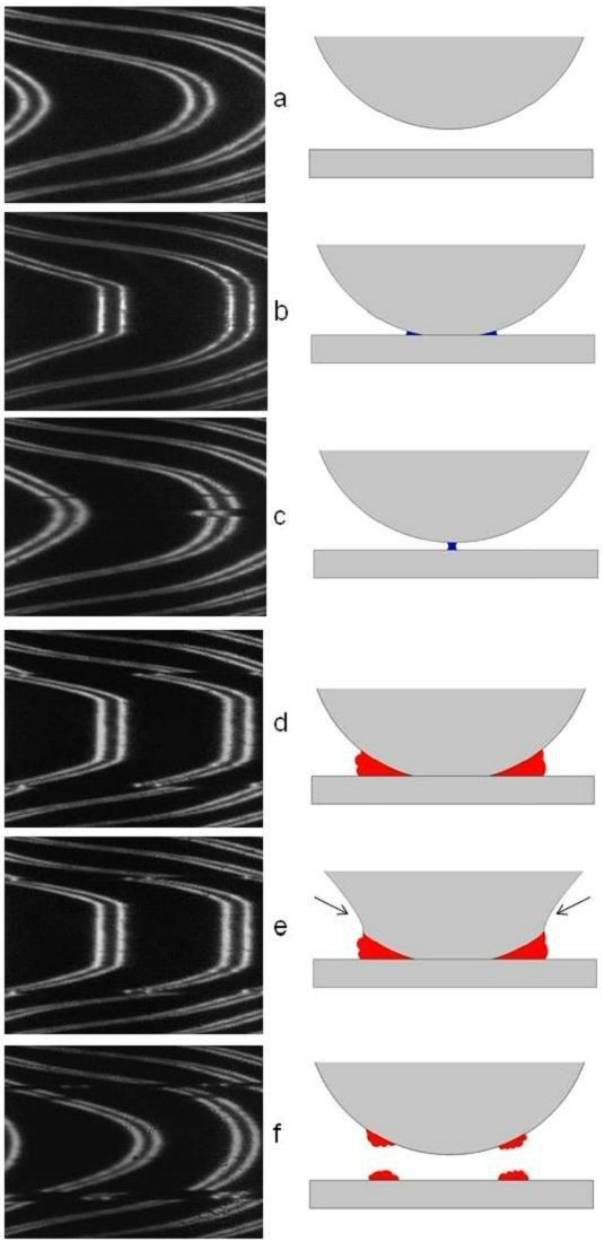

Figure 2 Interference fringes and the surface configuration deduced therefrom for mica surfaces in *neo*-pentanol vapour. The wavelength increases towards the left. The fringes are doublets due to the birefringence of mica, and their shape reflects the increasing surface separation on going away from the point of closest approach at the centre, and the surface flattening when the surfaces are in contact. Discontinuities can be seen where the refractive index changes abruptly for that of the vapour to the condensed phase. a) surfaces ca.50 nm apart in vapour, b) in contact in *neo*-pentanol vapour, c) after separation from contact with liquid bridge (a-c all at $\Delta T = 28$ K). d) surfaces in contact with solid annulus of $h \approx 200$ nm, e) surfaces deform as they are pulled apart (arrows), f) after large jump apart, showing solid residue on surfaces (d-f all at $\Delta T = 33$ K).

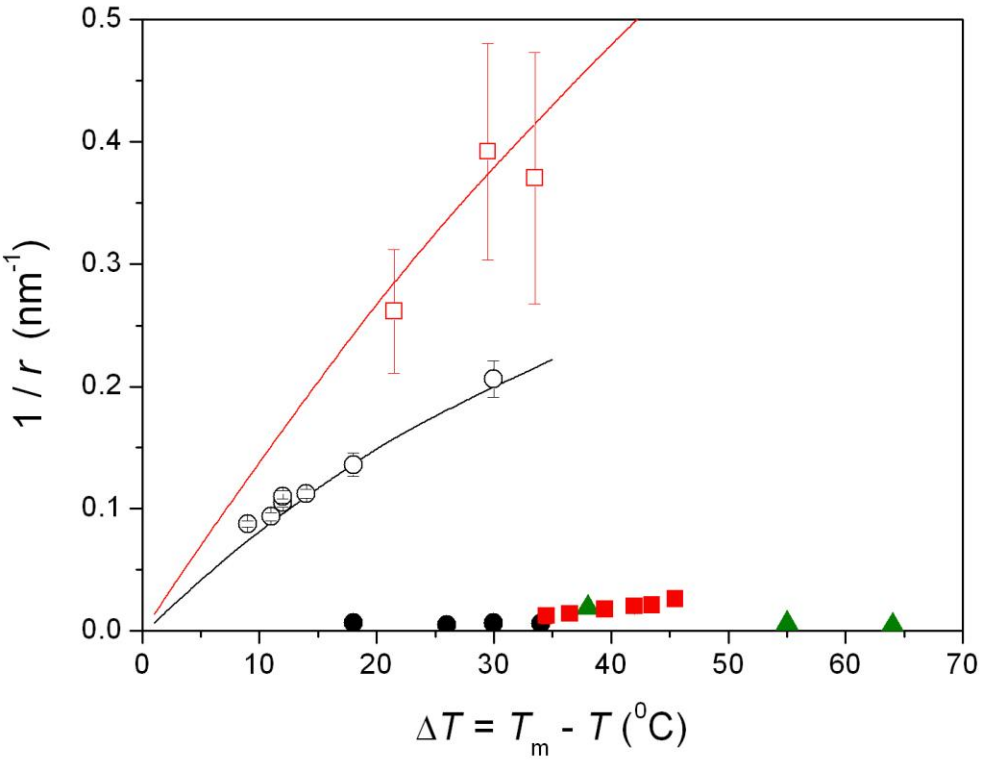

Figure 3 The inverse of the radius of curvature r (= (h-3t)/2) of the condensate-vapour interface for condensates of liquid *neo*-pentanol (open circles), liquid HMCTS (open squares), solid *neo*-pentanol (filled circles), solid HMCTS (filled squares) and solid norbornane (filled triangles) as a function of the temperature depression ΔT below the bulk melting point (i.e. temperature decreases towards the right). The full model (solid lines, see text) accounts well for the size of the liquid condensates, and note particularly the very significant increase in condensate size (decrease in 1/r) for solid condensates compared to liquid condensates. The temperature-dependence of the surface tension and the enthalpy of fusion cause the 1/r vs ΔT dependence to deviate from linearity as ΔT increases.

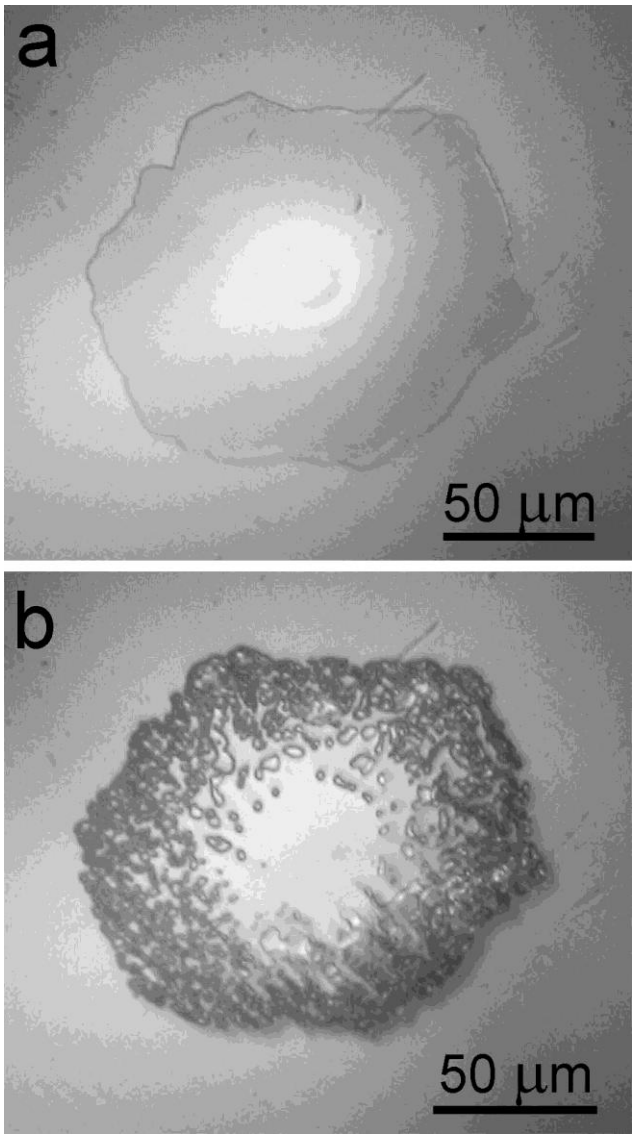

Figure 4 Microscope image taken from above of a solid norbornane deposit in the annular wedge between crossed mica cylinders (a) after nucleation in a liquid capillary condensate formed in saturated vapour at 52 K below the melting point. The bright centre region is mica-mica contact, and the norbornane vapour interface is an irregular hexagon. On separation the crystalline condensate joining the surfaces shatters (b).

REFERENCES

1. ten Wolde PR & Frenkel D (1997) Enhancement of Protein Crystal Nucleation by Critical Density Fluctuations. *Science* 277:1975-1978.
2. Yau S-T & Vekilov PG (2000) Quasi-planar nucleus Structure in Apoferritin Crystallisation. *Nature* 406:494-497.
3. Stradner A, *et al.* (2004) Equilibrium cluster formation in concentrated protein solutions and colloids. *Nature* 432:492-495.
4. Sear RP (2007) Nucleation: Theory and Applications to Protein Solutions and Colloidal Suspensions. *J. Phys. Cond. Matt.* 19:033101.
5. Erdemir D, Lee AY, & Myerson AS (2009) Nucleation of Crystals from Solution: Classical and Two-Step Models. *Acc. Chem. Res.* 42:621-629.
6. Savage JR & Dinsmore AD (2009) Experimental Evidence for Two-Step Nucleation in Colloidal Crystallisation. *Phys. Rev. Lett.* 102:198302.
7. Vekilov PG (2010) Nucleation. *Cryst. Growth Des.* 10:5007-5019.
8. Garetz BA, Matic J, & Myerson AS (2002) Polarization switching of crystal structure in the nonphotochemical light-induced nucleation of supersaturated aqueous glycine. *Phys. Rev. Lett.* 89:175501.
9. Kimura M (2006) Characterisationof the dense liquid precursor in homogeneous crystal nucleatin using solution state nuclear magnetic resonance spectroscopy. *Cryst. Growth Des.* 6:854-860.
10. Murray BJ, *et al.* (2010) Heterogeneous nucleation of ice particles on glassy aerosols under cirrus conditions. (Translated from English) *Nature Geoscience* 3:233-237 (in English).
11. Turnbull D (1950) Kinetics of Heterogeneous Nucleation. *J. Chem. Phys.* 18:198-203.
12. Scholl CA & Fletcher NH (1970) Decoration Criteria for Surface Steps. *Acta Met.* 18:1083-1086.
13. Nowak D & Christenson HK (2009) Capillary Condensation of Water between Mica Surfaces above and below Zero – Effect of Surface Ions. *Langmuir* 25:9908-9912.
14. Nowak D, Heuberger M, Zäch M, & Christenson HK (2008) Thermodynamic and Kinetic Supercooling of Liquid in a Wedge-pore. *J. Chem. Phys.* 129:154509.
15. Osthoff RC, Grubb WT, & Burkhard CA (1953) Physical properties of organosilicon compounds I. hexamethylcyclotrisiloxane and octamethylcyclotetrasiloxane. *J. Am. Chem. Soc.* 75:2227-2229.
16. Weast RC ed (1976) *Handbook of Chemistry and Physics* (CRC Press, Cleveland, OH), 57th Ed.
17. Faith WL, Keyes DB, & Clark RL eds (1957) *Industrial Chemicals* (Wiley & Sons, New York), pp 109-114.
18. Verevkin SP & Emel'yanenko VN (2004) The enthalpy of formation and strain of norbornane from thermochemical measurements and from *ab initio* calculations. *J. Phys. Chem. A* 108:6575-6580.
19. Christenson HK & Yaminsky VV (1993) Adhesion and Solvation Forces between Surfaces ion Liquids Studied by Vapor-Phase Experiments. *Langmuir* 9:2448-2454.
20. Wanless EJ & Christenson HK (1994) Interaction between Surfaces in Ethanol - Adsorption, Capillary Condensation and Solvation Forces. (Translated from English) *Journal of Chemical Physics* 101(5):4260-4267 (in English).
21. Christenson HK (1994) Capillary Condensation Due to Van Der Waals Attraction in Wet Slits. *Phys. Rev. Lett.* 73:1821.

22. Qiao Y & Christenson HK (1999) Triple-point wetting and liquid condensation in a slit pore. (Translated from English) *Physical Review Letters* 83(7):1371-1374 (in English).
23. Christenson HK (1996) Surface deformations in direct force measurements. (Translated from English) *Langmuir* 12(5):1404-1405 (in English).
24. Sill RC & Skapski AS (1957) Method for determining the surface tension of solids, from their melting points in thin wedges *J. Chem. Phys.* 24:644-651.
25. Murray BJ, *et al.* (2010) Kinetics of the Homogeneous Freezing of Water. *Phys. Chem. Chem. Phys.* 12:10380-10387.
26. Maeda N & Christenson HK (1999) Direct observation of surface effects on the freezing and melting of an n-alkane. *Colloids Surf. A: Physicochem. Eng. Aspects* 159:135-148.
27. Shaw RA, Durant AJ, & Mi Y (2005) Heterogenous surface crystallisation observed in undercooled water. *J. Phys. Chem. B* 109:9865.
28. Sear RP (2007) Nucleation at contact lines where fluid-fluid interfaces meet solid surface. *J. Phys. Cond. Matt.* 19:466106.
29. Fukuta N (1966) Activation of atmospheric particles as ice nuclei in cold and dry air. *J. Atmos. Sci.* 23:741-750.
30. Fletcher NH (1969) Active sites and ice crystal nucleation. *J. Atmos. Sci.* 26:1266-1271.
31. Chayen NE, Saridakis E, & Sear RP (2006) Experiment and theory for heterogeneous nucleation of protein crystals in a porous medium. *Proc. Nat. Acad. Sci.* 103:597-601.
32. Sugahara M, Asada Y, Morikawa Y, Kageyama Y, & Kunishima N (2008) Nucleant-Mediated Protein Crystallization with the Application of Microporous Synthetic Zeolites. *Acta Crystallographica Section D-Biological Crystallography* 64:686-695.
33. Diao Y, Harada T, Myerson AS, Hatton TA, & Trout BL (2011) The Role of Nanopore Shape in Surface-Induced Crystallization. *Nat. Mat.* 10:867-871.
34. van Meel JA, Sear RP, & Frenkel D (2010) Design Principles for Broad-Spectrum Protein-Crystal Nucleants with Nanoscale Pits. *Phys. Rev. Lett.* 105:205501.
35. Chen B, Kim H, Keasler SJ, & Nellas RB (2008) An Aggregation-Volume-Bias Monte Carlo Investigation on the Condensation of a Lennard-Jones Vapor below the Triple Point and Crystal Nucleation in Cluster Systems: An In-Depth Evaluation of the Classical Nucleation Theory. *J. Phys. Chem. B* 112:4067-4078.
36. van Meel JA, Page AJ, Sear RP, & Frenkel D (2008) Two-step vapor-crystal nucleation close below triple point. *J. Chem. Phys.* 129:204505.
37. Meldrum FC (2003) Calcium carbonate in biomineralisation and biomimetic chemistry. *International Materials Reviews* 48(3):187-224.
38. Wolf SE, *et al.* (2011) Carbonate-coordinated metal complexes precede the formation of liquid amorphous mineral emulsions of divalent metal carbonates. *Nanoscale* 3:1158-1165.
39. Wang YW, Kim Y-Y, Christenson HK, & Meldrum FC (2012) A new precipitation pathway for calcium sulfate dihydrate (gypsum) via amorphous and hemihydrate intermediates. . *Chem. Commun.* 48:504-506.
40. Curry JE & Christenson HK (1996) Adorption, wetting and capillary condensation of nonpolar fluids in mica slits. *Langmuir* 12:5729-5735.
41. Israelachvili JN (1973) Multiple-Beam Interferometry. *J. Colloid Interface Sci.* 44:259.
42. Evans R & Marini Bettolo Marconi U (1985) The role of wetting films in capillary condensation and rise: Influence of long-range forces. *Chem. Phys. Lett.* 114:415-422.